RIMS Kôkyûroku Bessatsu
B35 (2012), 115–124

One-Dimensional Anisotropic Surface Diffusion

By

Dieu Hung HOANG* and Michal BENEŠ**

Abstract

This contribution deals with the motion law of anisotropic surface diffusion of graphs which is an important concept in epitaxial growth (see [3]). The numerical scheme is based on the method of lines where the spatial derivatives are approximated by finite differences [1]. We implement the adaptive Runge-Kutta-Merson method for solving the semi-discrete scheme. Finally, we show computational results with various anisotropy settings.

Introduction

Crystallization is the process where solid crystals are formed from melt, solution, or vapour phase. There are two major stages involved in the crystallization process – *nucleation* and *crystal growth*. Nucleation is the stage where crystal forming units (atoms, ions, or molecules) gather into clusters which are unstable until they reach a critical size. Stable clusters are then called nuclei. After nuclei are created, crystal growth begins. This is the stage where new crystal forming units are incorporated into the crystal lattice. Seed crystals may be used to bypass the nucleation stage; thus, the growth can start immediately.

In this contribution we deal with the growth of a thin film of single crystal material on a single crystal substrate so that the film has the same structure as the substrate, known as epitaxy. Here, the substrate functions as a seed crystal. According to the theory of Burton, Cabrera, and Frank [2] atoms are first adsorbed to the crystalline surface, where they are called adatoms, and then they diffuse freely along the surface. Finally they can detach from or attach to the crystal (see Fig. 1), and the deposited film takes on a lattice structure and orientation identical to those of the substrate.

Received October 16, 2011. Revised October 9, 2012.
2000 Mathematics Subject Classification(s):
Key Words: anisotropic surface diffusion, method of lines, FDM, heteroepitaxy, ATG instability
*Department of Mathematics, Faculty of Nuclear Sciences and Physical Engineering, Czech Technical University in Prague, Prague, Czech Republic.
e-mail: dieu.hung.hoang@fjfi.cvut.cz
**Department of Mathematics, Faculty of Nuclear Sciences and Physical Engineering, Czech Technical University in Prague, Prague, Czech Republic.
e-mail: michal.benes@fjfi.cvut.cz

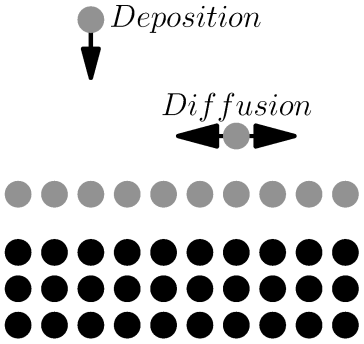

Figure 1: Atomistic view of the basic processes in epitaxy.

In general we distinguish two cases: homoepitaxy and heteroepitaxy. While in homoepitaxy the film and substrate are made of the same material, in heteroepitaxy the film is made of a material different from the substrate. One example of heteroepitaxy is the growth of germanium film on a silicon substrate. The lattice parameter of the film differs from the substrate (less then 4% for Ge/Si). Hence strains are introduced into the heteroepitaxial film. Due to the effects of stress, the flat film surface is unstable to small perturbations and such films can undergo a morphological instability, known as the Asaro-Tiller-Grinfeld (ATG) instability.

Fig. 2 illustrates the physical mechanism of the ATG instability [7]. The surface tends to remain flat to get the lowest surface free energy (Fig. 2a). But, if elastic energy is present in the film, the corrugated surface has lower elastic energy than the flat one (Fig. 2b). In such a case, the elastic energy is lowered by elastic deformation so that the film breaks into isolated islands (called quantum dots). Therefore, quantum dots are caused by the competition between surface and elastic energies; elastic energy is reduced as the surface area increases. Here, the mass is transported by surface diffusion.

Quantum dots have interesting electrical and optical properties, and their sizes range from several to hundreds of nanometers. Quantum dots are widely used in optical and optoelectronic devices, quantum computation, and biology. Hence, accurate knowledge of morphological changes in epitaxial thin films is crucial for governing the material's properties in applications.

A number of continuum models have been developed for modelling heteroepitaxial growth. A continuum model was derived for the evolution of an epitaxially strained dislocation-free solid film on a rigid substrate by Spencer et al. [6] and on a deformable substrate by Tekalign and Spencer [8]. Xiang and E [9] derived a nonlinear approximation equation for the surface morphology of an infinitely thick stressed solid in 2D.

Our goal is to provide a suitable computational tool for studying such phenomena.

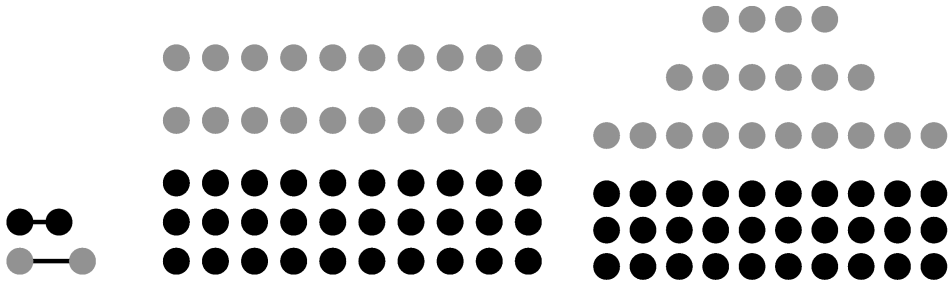

(a) High energy. (b) Low energy.

Figure 2: ATG instability.

§ 1. Evolution problem

In this contribution, we deal with the motion law of anisotropic surface diffusion in two dimensions

$$V = \Delta_\Gamma(F - H) \text{ on } \Gamma, \tag{1.1}$$

where Γ is the curve in $\mathbb{R}^2$, V is the normal velocity of Γ, Δ_Γ is the Laplace-Beltrami operator with respect to Γ, H is the anisotropic mean curvature given by a prescribed anisotropy, and F is the forcing term. In what follows we shall study the surface evolution as the graph of the height function.

In order to incorporate the anisotropy into the model we replace the isotropic Euclidean norm in $\mathbb{R}^2$ by another norm exhibiting the desired anisotropy. Following [4] we consider a nonnegative function $\Phi : \mathbb{R}^2 \to \mathbb{R}_0^+$ which is smooth, strict convex, $\mathcal{C}^2(\mathbb{R}^2\backslash\{0\})$ and satisfying

$$\begin{aligned} &\Phi(t\eta) = |t|\Phi(\eta), \quad t \in \mathbb{R}, \quad \eta \in \mathbb{R}^2, \\ &\lambda|\eta| \le \Phi(\eta) \le \Lambda|\eta|, \end{aligned}$$

where $\lambda, \Lambda > 0$. The function given by

$$\Phi^0(\eta^*) = \sup\{\eta^* \cdot \eta | \Phi(\eta) \le 1\}$$

is its dual. They satisfy the relations

$$\begin{aligned} \Phi^0_\eta(t\eta^*) = \frac{t}{|t|}\Phi^0_\eta(\eta^*), \qquad \Phi^0_{\eta\eta}(t\eta^*) = \frac{1}{|t|}\Phi^0_{\eta\eta}(\eta^*), \qquad t \in \mathbb{R} - \{0\}, \\ \Phi(\eta) = \Phi_\eta(\eta) \cdot \eta, \qquad \Phi^0(\eta^*) = \Phi^0_\eta(\eta^*) \cdot \eta^*, \ \eta, \eta^* \in \mathbb{R}^2, \end{aligned}$$

where the index η means the derivative with respect to η (i.e., $\Phi^0_\eta = (\partial_{\eta_1}\Phi^0, \partial_{\eta_2}\Phi^0)$). We define the map $T^0 : \mathbb{R}^2 \to \mathbb{R}^2$ as

$$\begin{aligned} &T^0(\eta^*) := \Phi^0(\eta^*)\Phi^0_\eta(\eta^*) \quad \text{for } \eta^* \neq 0, \\ &T^0(0) := 0. \end{aligned}$$

It allows to define the Φ-gradient of a smooth function u as follows

$$\nabla_\Phi u := T^0(\nabla u) = \Phi^0(\nabla u)\Phi^0_\eta(\nabla u) = [T^0_1(\nabla u), T^0_2(\nabla u)],$$

where $\nabla = [\partial_x, \partial_y]$. We assume that there is a function $P : \mathbb{R}^{1+1} \to \mathbb{R}$ such that

$$\Gamma(t) = \{[x, y] \in \mathbb{R}^2 \mid y = P(t, x) \in (a, b)\}.$$

Let $U(x, y) = P(t, x) - y = 0$. Then the anisotropic mean curvature is given by

$$\begin{aligned} H &= \nabla \cdot \left(\frac{\nabla_\Phi U}{\Phi^0(\nabla U)} \right) = \nabla \cdot \left(\frac{T^0(\nabla U)}{\Phi^0(\nabla U)} \right) = \nabla \cdot \left(\frac{T^0(\partial_x P, -1)}{\Phi^0(\partial_x P, -1)} \right) \\ &= \partial_x \left(\frac{T^0_1(\partial_x P, -1)}{\Phi^0(\partial_x P, -1)} \right). \end{aligned}$$

Other quantities are expressed as follows

$$\begin{aligned} Q(\partial_x P) &= \sqrt{1 + |\partial_x P|^2} && \text{(area element)}, \\ \mathbf{N} = [N, N_2] &= \left[\frac{\partial_x P}{Q(\partial_x P)}, \frac{-1}{Q(\partial_x P)} \right] && \text{(normal vector)}, \\ V &= \frac{1}{Q(\partial_x P)} \frac{\partial P}{\partial t} && \text{(normal velocity)}. \end{aligned}$$

By substituting these quantities into the Eq. (1.1) we obtain the evolution equations

$$\frac{\partial P}{\partial t} = \partial_x (Q(\partial_x P)(\partial_x (F - H) - (\partial_x (F - H) \cdot N)N)) \text{ on } (a, b) \times (0, T), \tag{1.2}$$

$$H = \partial_x \left(\frac{T^0_1(\partial_x P, -1)}{\Phi^0(\partial_x P, -1)} \right) \quad \text{on } (a, b) \times (0, T). \tag{1.3}$$

The boundary and initial conditions are given by

$$\partial_x P = 0, \quad \partial_x H = 0 \quad \text{on } \{a, b\} \times (0, T), \tag{1.4}$$

$$P|_{t=0} = P_{ini} \quad \text{on } [a, b]. \tag{1.5}$$

§ 2. Numerical solution

The numerical scheme is based on the method of lines. The spatial derivatives are first discretized and the time variable is left continuous. This leads to a system of ordinary differential equations (ODEs) which can be solved by the adaptive Runge-Kutta-Merson method (see [5]). We consider the computational domain (a, b) and introduce

the following notation:

$$\begin{aligned}
h &= \frac{b-a}{N} && \text{(mesh size)},\\
u_i &= u(a+ih), &&\\
\omega_h &= \{a+ih | i=1,...,N-1\} && \text{(grid of internal nodes)},\\
\bar{\omega}_h &= \{a+ih | i=0,...,N\} && \text{(grid of all nodes)},\\
\gamma_h &= \{a,b\}, &&\\
u_{x,i} &= \frac{u_{i+1}-u_i}{h} && \text{(forward difference)},\\
u_{\bar{x},i} &= \frac{u_i-u_{i-1}}{h} && \text{(backward difference)},\\
\mathcal{P}_h g &= g|_{\bar{\omega}_h} && \text{(projection operator)}.
\end{aligned}$$

Then we propose a semi-discrete scheme [4]

$$\frac{\partial P^h}{\partial t} = (Q(P^h_{\bar{x}})((F-H^h)_{\bar{x}} - ((F-H^h)_{\bar{x}} \cdot N^h)N^h))_x, \tag{2.1}$$

$$H^h = \left(\frac{T_1^0(P^h_{\bar{x}},-1)}{\Phi^0(P^h_{\bar{x}},-1)}\right)_x, \quad N^h = \frac{P^h_{\bar{x}}}{Q(P^h_{\bar{x}})}. \tag{2.2}$$

The boundary and initial conditions are written as follows

$$P^h_{\bar{x},0} = P^h_{\bar{x},N} = 0, \quad H^h_{\bar{x},0} = H^h_{\bar{x},N} = 0 \quad \text{in } (0,T), \tag{2.3}$$

$$P^h\big|_{t=0} = \mathcal{P}_h P_{ini} \quad \text{on } \bar{\omega}_h. \tag{2.4}$$

The scheme (2.1) can be rewritten in the form

$$\frac{\mathrm{d}P^h}{\mathrm{d}t} = f(t,P^h).$$

Then, the algorithm of the Runge-Kutta-Merson method for solving this system is described in Algorithm 1.

§ 3. Numerical results

In this section we present several numerical results with various anisotropy settings. We shall explore the long-time behaviour of Eq. (1.1). In all computations, we consider the domain $(0,2)$, the step size $h = 0.01$, and the forcing term $F = -100/P$.

Example 1. We consider the initial condition $P_{ini}(x) = 1 + 0.1\cos(12\pi x)$ and $\Phi^0(-\nabla P, 1) = \sqrt{(\nabla P)^2 + 1}$. The solution at different times is displayed in the Fig. 3 which shows an evolution towards island formation. Here, the solution is first smoothed out and then an array of islands is created.

Algorithm 1 Runge-Kutta-Merson method

1. Compute the coefficients

$$\begin{aligned}
k_{1,i} &= \tau f(t, P^h)_i, \\
k_{2,i} &= \tau f\left(t + \frac{\tau}{3}, P^h + \frac{\tau}{3}k_1\right)_i, \\
k_{3,i} &= \tau f\left(t + \frac{\tau}{3}, P^h + \frac{\tau}{6}k_1 + \frac{\tau}{6}k_2\right)_i, \\
k_{4,i} &= \tau f\left(t + \frac{\tau}{2}, P^h + \frac{\tau}{8}k_1 + \frac{3\tau}{8}k_3\right)_i, \\
k_{5,i} &= \tau f\left(t + \tau, P^h + \frac{\tau}{2}k_1 - \frac{3\tau}{2}k_3 + 2\tau k_4\right)_i
\end{aligned}$$

   for $i = 0, \ldots, N$.

2. Evaluate the local truncation error

$$E = \max_{i=0,\ldots,N} \left\{ \frac{|2k_1 - 9k_3 + 8k_4 - k_5|}{30} \right\}$$

3. If $E < \epsilon$ then compute

$$\begin{aligned}
t &= t + \tau, \\
P_i^h &= P_i^h + \frac{1}{6}\left(k_{1,i} + 4k_{4,i} + k_{5,i}\right) \text{ for } i = 0, \ldots, N.
\end{aligned}$$

4. Update the step size

$$\tau = 0.8\tau \left(\frac{\epsilon}{E}\right)^{0.2}.$$

Example 2. We consider $\Phi^0(-\nabla P, 1) = \sqrt{0.5(\nabla P)^2 + 1}$ and the same initial condition as in the example 1. In this example, we observe the early smoothing effect too but the density of islands is larger than the density in the previous example (see Fig. 4).

Example 3. For $\Phi^0(-\nabla P, 1) = \sqrt{0.1(\nabla P)^2 + 1}$ and the same initial condition as in the previous examples we do not observe the smoothing effect. On the contrary, from the beginning and evolve towards crack formation (see Fig. 5).

Example 4. Fig. 6 displays solutions with another initial condition and various anisotropy settings.

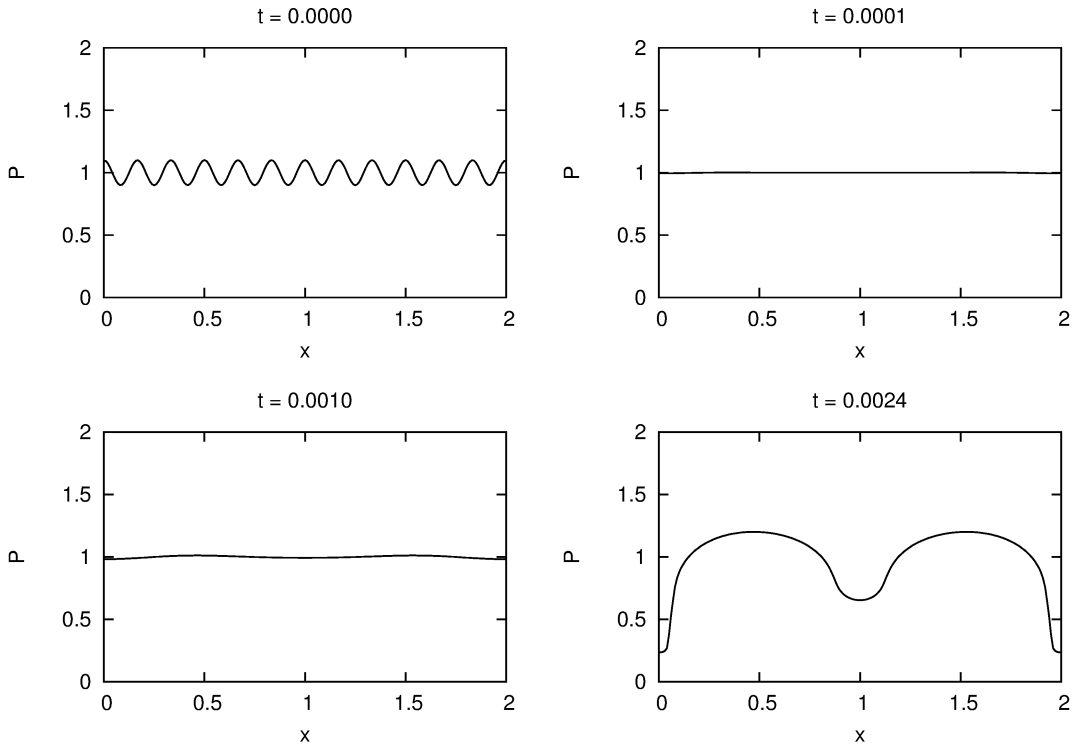

Figure 3: Example 1. Solutions for $\Phi^0(-\nabla P, 1) = \sqrt{(\nabla P)^2 + 1}$ at different times.

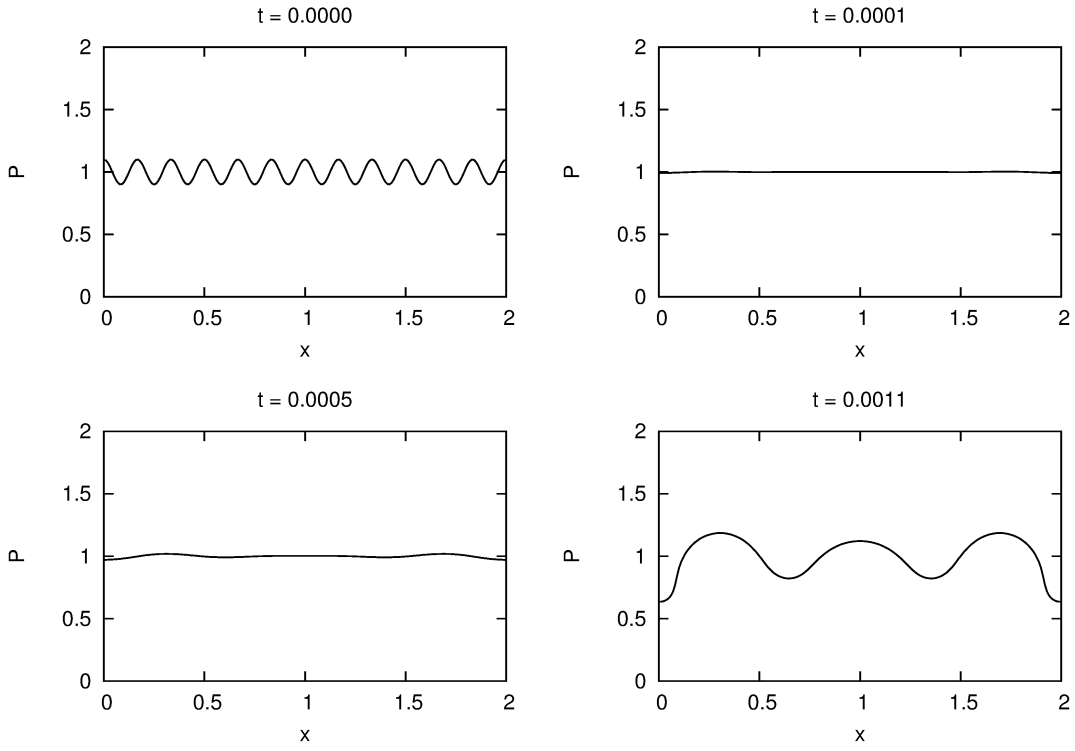

Figure 4: Example 2. Solutions for $\Phi^0(-\nabla P, 1) = \sqrt{(0.5\nabla P)^2 + 1}$ at different times.

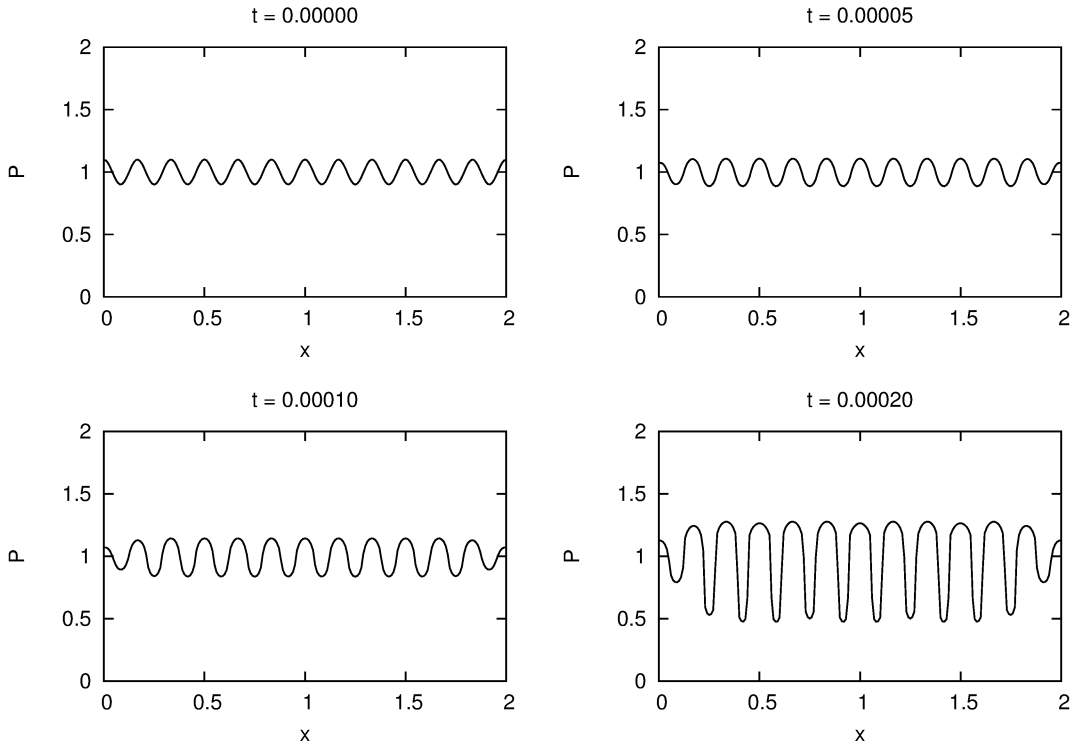

Figure 5: Example 3. Solutions for $\Phi^0(-\nabla P, 1) = \sqrt{0.1(\nabla P)^2 + 1}$ at different times.

§ 4. Conclusion

The influence of surface energy anisotropy on the dynamics of heteroepitaxial growth has been studied by the method of lines combined with the finite difference method. The Runge-Kutta-Merson method for solving a system of ODEs is reliable and its use for the anisotropic surface diffusion has been described. Finally, we have shown several computational experiments.

Acknowledgement

This work was partially supported by the project "Applied Mathematics in Technical and Physical Sciences" of the Ministry of Education, Youth and Sports of the Czech Republic No. MSM 6840770010 and by the project "Advanced Supercomputing Methods for Implementation of Mathematical Models" of the Student Grant Agency of the Czech Technical University in Prague No. SGS11/161/OHK4/3T/14.

References

[1] M. BENEŠ, *Diffuse-Interface Treatment of the Anisotropic Mean-Curvature Flow*, Applications of Mathematics, 48 (2003), pp. 437–453.

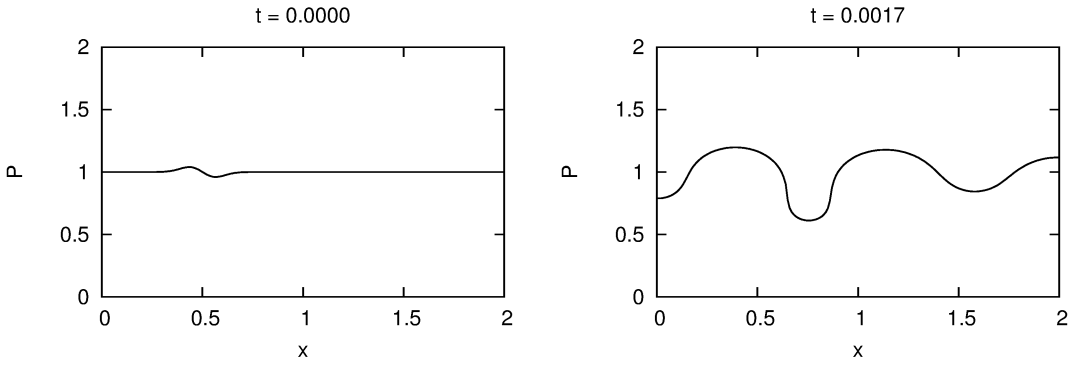

(a) Initial condition. (b) $\Phi^0(-\nabla P, 1) = \sqrt{(\nabla P)^2 + 1}$.

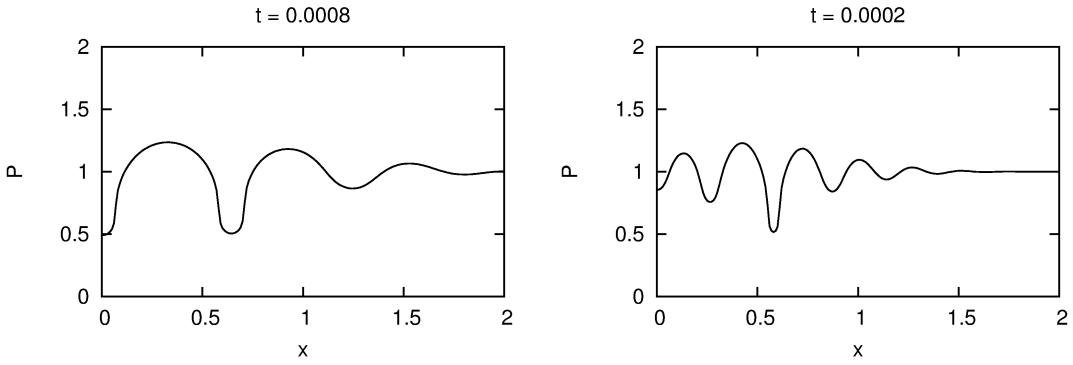

(c) $\Phi^0(-\nabla P, 1) = \sqrt{0.5(\nabla P)^2 + 1}$. (d) $\Phi^0(-\nabla P, 1) = \sqrt{0.1(\nabla P)^2 + 1}$.

Figure 6: Example 4

[2] W. K. Burton, N. Cabrera, and F. C. Frank, *The Growth of Crystals and the Equilibrium Structure of their Surfaces*, Phil. Trans. R. Soc., 243 (1951), pp. 299–358.

[3] M. E. Gurtin and M. E. Jabbour, *Interface Evolution in Three Dimensions with Curvature-Dependent Energy and Surface Diffusion: Interface-Controlled Evolution, Phase Transitions, Epitaxial Growth of Elastic Films*, Archive for Rational Mechanics and Analysis, 163 (2002), pp. 171–208.

[4] D. H. Hoang and M. Beneš, *Numerical Simulation of Anisotropic Surface Diffusion*, in Numerical Mathematics and Advanced Applications 2011 - Proceedings of ENUMATH 2011, the 9th European Conference on Numerical Mathematics and Advanced Applications, Leicester, September 2011, A. Cangiani, R. L. Davidchack, E. H. Georgoulis, A. Gorban, J. Levesley, and M. V. Tretyakov, eds., to appear.

[5] M. Holodniok, A. Klíč, M. Kubíček, and M. Marek, *Methods of Analysis of Nonlinear Dynamical Models*, Academia Praha, 1986.

[6] B. J. Spencer, S. H. Davis, and P. W. Voorhees, *Morphological instability in epitaxially strained dislocation-free solid films: Nonlinear evolution*, Physical Review B, 47 (1993), pp. 9760–9777.

[7] D. J. Srolovitz, *On the stability of surfaces of stressed solids*, Acta Metallurgica, 37 (1989), pp. 621–625.

[8] W. T. Tekalign and B. J. Spencer, *Evolution equation for a thin epitaxial film on a*

deformable substrate, Journal of Applied Physics, 96 (2004), pp. 5505–5512.

[9] Y. XIANG AND W. E, *Nonlinear evolution equation for the stress-driven morphological instability*, Journal of Applied Physics, 91 (2002), pp. 9414–9423.